ELSEVIER

Polymer 40 (1999) 3345–3351

polymer

Crystallite modulus of double-stranded helices of isotactic poly(methyl methacrylate): the X-ray measurement and the theoretical calculation

Sebastien Urbanek[a], Kohji Tashiro[b,*], Tatsuki Kitayama[a], Koichi Hatada[a]

[a]*Department of Chemistry, Graduate School of Engineering Science, Osaka University, Toyonaka, Osaka 560, Japan*
[b]*Department of Macromolecular Science, Graduate School of Science, Osaka University, Toyonaka, Osaka 560, Japan*

Received 14 May 1998; received in revised form 30 June 1998; accepted 23 July 1998

Abstract

The Young's modulus or crystallite modulus of ca. 10 GPa has been obtained experimentally by the X-ray diffraction method for isotactic poly(methyl methacrylate) (*it*-PMMA) crystal along the chain direction. The modulus, calculated by the energy minimization method, for the double-stranded helix model of *it*-PMMA was 19 GPa, which was about twice as high as that of the single helix model, 11 GPa. This calculation indicated clearly a role for the intertwining of the two chains on the mechanical toughening of the polymer crystal along the chain axis, although the calculated value was an overestimation compared with the observed value. © 1999 Elsevier Science Ltd. All rights reserved.

Keywords: Isotactic poly(methyl methacrylate); Crystallite modulus; X-ray diffraction

1. Introduction

Recently the crystal structure of isotactic poly(methyl methacrylate) (*it*-PMMA) has been proposed. Although several types of structural models have been reported [1–8], one of the most plausible models may be that described by Kusanagi et al. [5,8]. In their proposed structure, double-stranded helices of *it*-PMMA are packed in an orthorhombic lattice cell with the parameters $a = 20.98$ Å, $b = 12.17$ Å and c (fiber axis) $= 10.50$ Å. Two polymer chains of 10/1 helix are intertwined to form a double helix with a repeating period of c. These two chains are combined together, mainly by non-bonded van der Waals interactions.

It is important to study the effect of this association of two chains in a double-stranded helix on the mechanical properties of *it*-PMMA, with an emphasis on the elastic constant along the chain direction. In the present study, we measured the crystallite modulus or limiting modulus of *it*-PMMA by the X-ray diffraction method. The experimental value thus obtained was interpreted from the viewpoint of structure and interaction through the computer simulation.

This may be the first report on successfully evaluating the crystallite modulus of double-stranded *it*-PMMA chains, both experimentally and theoretically. Since PMMA is one of the basically important polymers, the crystallite modulus obtained in this study might play some significant role in the discussion of the mechanical properties of bulk PMMA samples.

2. Experimental

2.1. Preparation of oriented it-PMMA samples

The *it*-PMMA samples used in this study were anionically prepared in toluene with *t*-C_4H_9MgBr. The reagent purification, the polymerization procedure and the recovery of the polymers are described in detail in Ref. [9]. To obtain high-molecular-weight PMMA samples suitable for the present work, the polymerizations were carried out at -60°C to compensate for the slow rate of polymerization. Methyl methacrylate was added slowly to a solution of *t*-C_4H_9MgBr in toluene at -60°C under a nitrogen atmosphere. The number-average molecular weight (M_n) of the polymer was adjusted by selecting the proper ratio of monomer to initiator. Termination of the polymerization was done by adding acidified methanol to the polymerization mixture at the polymerization temperature. *it*-PMMA was recovered by precipitating the mixture into hexane and water successively. The characterizations of the prepared samples are listed in Table 1.

* Corresponding author.

PII: S0032-3861(98)00567-9

Table 1
Characterization of the synthesized PMMA

Sample code	$\bar{M}_n$ [a] (n.m.r.)	$\bar{M}_w/\bar{M}_n$ [b]	Tacticity (%)[c]		
			mm	mr	rr
*it*710	70600	4.1	92.2	5.2	2.6
*it*712	361000	2.1	94.4	2.4	3.2

[a]Determined from the relative peak intensity of the *t*-butyl end group and methoxy group by ^{1}H n.m.r.
[b]Both PMMA samples showed bimodal GPC curves owing to the high viscosity of the polymerization media which disturbs the homogeneity of the polymerization system.
[c]Determined by ^{1}H n.m.r.

The *it*-PMMAs showed bimodal molecular weight distribution (MWD). Although polymerization of MMA with *t*-C_4H_9MgBr at -78°C usually gives a narrow MWD, the polymerization at -60°C and at high monomer/initiator ratio often gives polymers with a bimodal MWD, probably due to the existence of a small amount of active species with much higher reactivity (less than 1%). A similar phenomenon of coexistence of active species with different reactivities was observed in the polymerization of ethyl methacrylate with *t*-C_4H_9MgBr [10]. To suppress the formation of the active species with higher reactivity, effects of some additives such as Lewis acids are now being examined.

The *it*-PMMA powder was processed by compression molding in a hydraulic press at 180°C. First, it was allowed to stand between the press plates for 5 min; then it was pressed at about 50 kgf cm^{-2} for 2 min. The 0.5 mm thick plate thus obtained was quenched in iced water. A small platelet of 1–2 mm width was cut from this plate and stretched in water at 70°C to different draw ratios. The annealing conditions of such an uniaxially oriented sample are given in the sections concerned.

2.2. X-ray measurement under tension

An X-ray apparatus with a two-dimensional imaging plate detector (DIP1000, MAC Science Co. Ltd, Japan) was used for X-ray diffraction measurements. The X-ray radiation was a graphite-monochromatized Mo–Kα line with a wavelength of 0.7107 Å.

The experimental equipment for the measurement of crystallite modulus is schematically represented in Fig. 1 [11]. The oriented sample was set horizontally with one end fixed to a load cell that could evaluate the force applied to the sample, and with another connected to a weight through a set of pulleys.

The meridional reflection 005 was employed for the measurement of the stress-induced change of the repeating period along the chain axis. *it*-PMMA should exhibit the many other meridional reflections in addition to the 005 reflection. There were several reasons why this 005 reflection was employed here. As seen in Figs 2 and 3, the 005 reflection is broad and relatively weak compared with the other equatorial reflections, leading us to predict that the higher-angle meridional reflections might be much broader and weaker and so the accuracy to trace the change in the reflectional position might be much lower. For an accurate determination of the shift of the meridional reflection, an aluminum powder was pasted on the sample and a correction of the scattering angle was made. The two weak reflections from the aluminum powder were found to overlap with the 005 reflection of the sample. This overlap might cause the lowering of the accuracy in evaluating the exact peak position change. But we found that this overlap might be utilized rather positively: the curve separation could be performed well by adjusting the peak positions and the relative

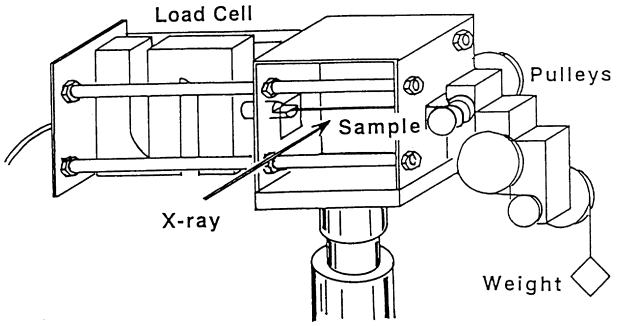

Fig. 1. Stretching apparatus for the X-ray measurement of the crystallite modulus of polymers.

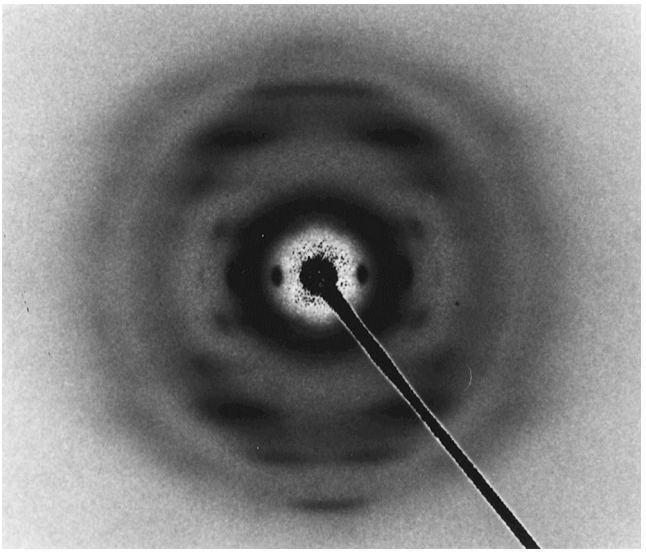

Fig. 2. X-ray fiber pattern of the uniaxially-oriented and annealed *it*-PMMA sample.

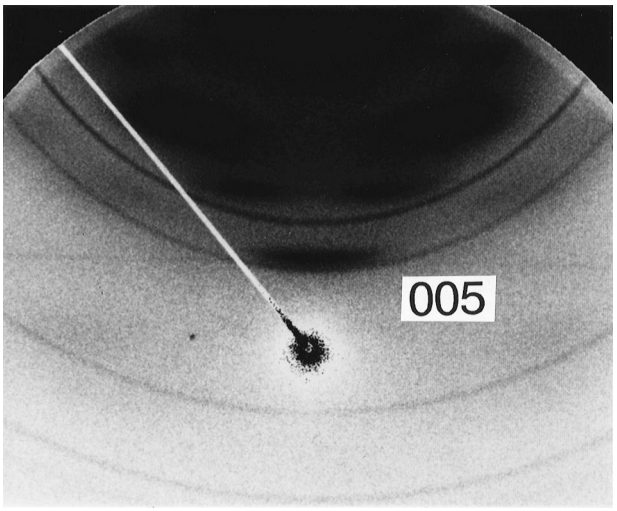

Fig. 3. Meridional reflection 005 measured for the uniaxially-oriented and annealed *it*-PMMA sample, where the sample is tilted by 9.8° from the initial direction.

intensity of these two aluminum reflections, which should be common through the measurements.

3. Results and discussion

3.1. Evaluation of crystallite modulus

Fig. 2 shows the X-ray pattern observed for an uniaxially stretched sample (draw ratio 10) annealed at 110°C for 49 h at constant length. In this figure, the vertical direction is parallel to the chain axis. The degree of chain orientation is relatively high, allowing us to identify the meridional reflections clearly. For the evaluation of the crystallite modulus along the chain direction, the 005 reflection with the Bragg angle 19.5° was utilized. The imaging-plate pattern centered on this reflection is shown in Fig. 3, where the sample was tilted by ca. 9.8° from the initial direction and the imaging plate detector was rotated by 19.5° in the horizontal plane. In the actual measurement of the modulus, the sample was set to the stretching machine as illustrated already in Fig. 1.

The principle of the measurement is briefly explained below [11–13]. It consists of observing the shift of the 005 meridional reflection for the sample subjected to constant stress in the direction of the chain orientation. The crystal strain, ε, can be evaluated from the variation of the lattice distance, d_{005}, as follows:

$$\varepsilon = \Delta d_{005}/d_{005} = -(1/2)\cot(\theta_{005})\Delta(2\theta)_{005} \quad (1)$$

where Δd_{005} and $\Delta(2\theta)_{005}$ are the changes in the lattice spacing and the corresponding Bragg's angle, respectively. Fig. 4 shows the evolution of the peak position corresponding to the 005 reflection. The peak profiles were obtained by integrating the two-dimensional reflections along the direction parallel to the chain axis as a function of the Bragg angle (see Fig. 3). Each peak corresponds to a particular tensile stress applied to the sample.

The X-ray beam is not perfectly monochromatized but contains two components, Kα_1 and Kα_2, of wavelengths 0.7135 Å and 0.7093 Å, respectively. Therefore, strictly speaking, a shoulder may be present because of the second component, Kα_2 [11]. But the Bragg's angle $(2\theta)_{005}$ is not so high, ca. 19.5° for the Mo–Kα line, as to give the separation of these two components. Another possible contribution to the shoulder is the overlap of other neighboring reflections, for example the reflection of the aluminum powder pasted on the sample. These overlaps can be separated by carrying out a curve fitting. The result of the curve fitting is shown in Fig. 5. The shift of the component of interest is reproduced in Fig. 6. The shift of the Bragg angle is evaluated and the lattice strain along the chain direction is calculated from Eq. (1). Concerning the stress, it is assumed that the stress applied to the bulk sample is equal to the stress working on the crystalline region (the mechanical series model) [11–15]. The stress-strain data thus obtained are plotted in Fig. 7. The observed points can be fitted by a straight line passing through the origin, the slope of which gives the apparent crystallite modulus, ca. 10.1 ± 1.6 GPa.

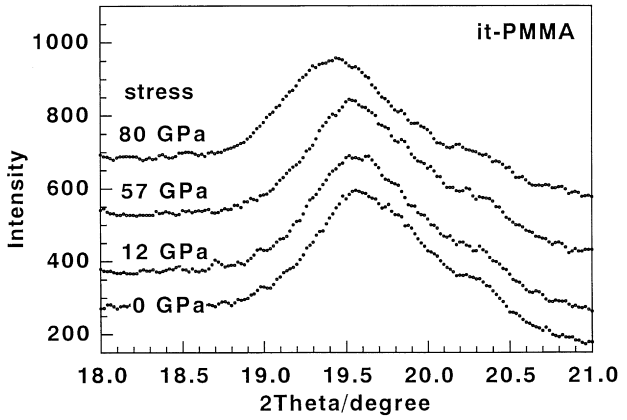

Fig. 4. Evolution of the observed peak profile of the 005 reflection under stress.

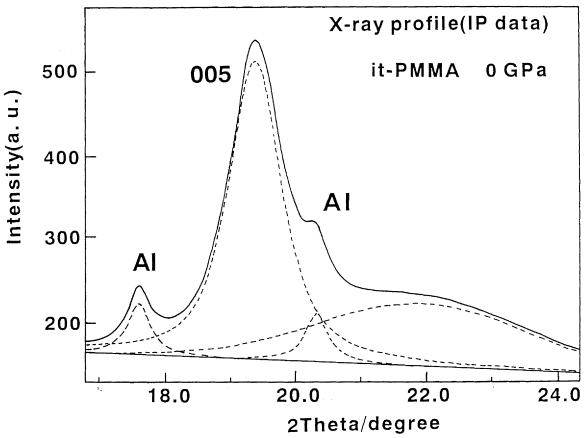

Fig. 5. Separation of the overlapped peaks.

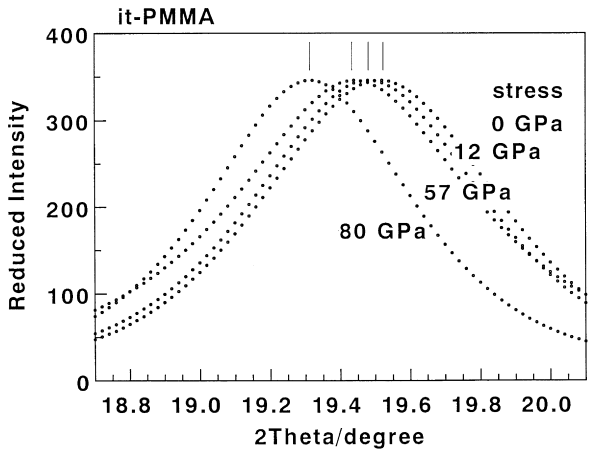

Fig. 6. Stress dependence of the 005 reflection extracted after the curve fitting.

At this point, we should check the reasonableness of our experimental assumption that the stress applied to the crystal is equal to the bulk stress; if not, this might significantly affect the observed modulus [11–15]. As described in the experimental section, the sample used here happened to be of bimodal MWD type. This might affect the stress distribution among the crystalline regions. But we cannot discuss this problem here because we do not have enough data concerning the morphology of the measured samples [14,15]. As a future problem we should check the effect of a bimodal MWD on the evaluated Young's modulus by measuring the stress-strain curve for the samples with an unimodal MWD. We might expect similar moduli for these two kinds of samples, as confirmed thoroughly for many kinds of polymer samples with various treatment histories [12,13]. The crystallite modulus obtained for *it*-PMMA is in the order characteristic of the helical chain conformation; 2.6 GPa for poly(trimethylene terephthalate) [16], 27 GPa for the γ form of nylon 6 [17], 40 GPa for isotactic polypropylene [12,13,18,19] and so on.

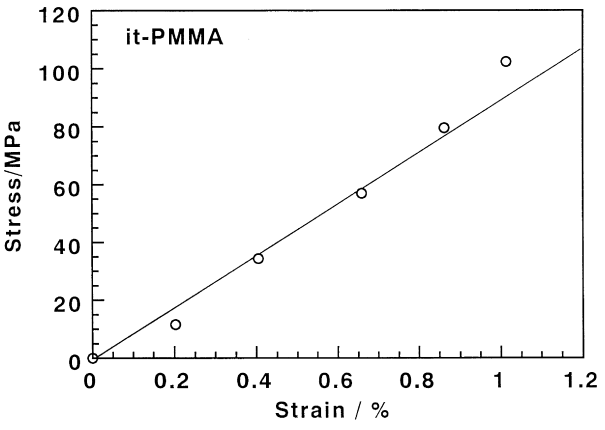

Fig. 7. Stress-strain plot obtained for the *it*-PMMA crystal along the chain axis.

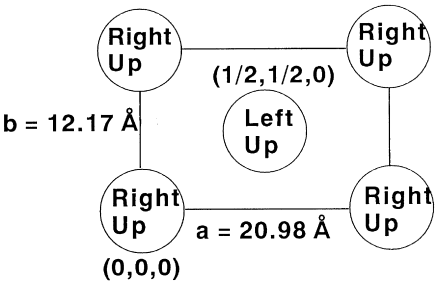

Fig. 8. Starting model used in the energy minimization of the crystal structure of *it*-PMMA [8].

3.2. Computer simulation

In order to interpret the crystallite modulus obtained by the X-ray measurement, calculations of the three-dimensional elastic constants were performed.

3.2.1. Energy minimization

The crystal structure of *it*-PMMA reported by Kusanagi et al. [8] was used as the starting model for the energy minimization procedure. Although their model has not yet been uniquely determined, we adopted the structure shown in Fig. 8 as one possibility. The cell belongs to the space group Pba2, with the parameters $a = 20.98$ Å, $b = 12.17$ Å, c (fiber axis) $= 10.50$ Å and $\alpha = \beta = \gamma = 90°$. The molecular conformation of a single chain is a 10/1 helix with the skeletal torsional angles of $\tau_1 = -179°$ and $\tau_2 = -148°$, where τ_1 and τ_2 are defined as below:

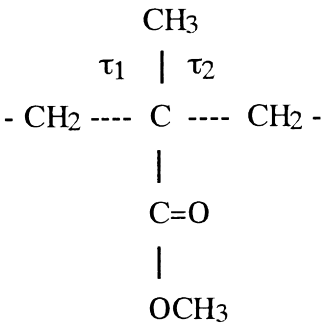

As shown in Fig. 8, the double-stranded helices are located at the corner and center positions of the lattice. They are packed in the same direction along the chain axis but with inversed helicity.

The construction of the model was made by utilizing the commercially available software of Polymer (Version 3.0.0) and Cerius^2 (Version 2.0) of Molecular Simulations Inc., USA. The energy minimization was carried out with the universal force field [20] at an energy conversion condition of 0.001 kcal mol^{-1}. The lattice parameters were allowed to be varied during the energy minimization procedure. The atomic charges were calculated by the method proposed by Gasteiger and Marsili [21] and the Coulombic interaction energy was evaluated by the Ewald method: the charges were assigned to the atoms in the

following way:

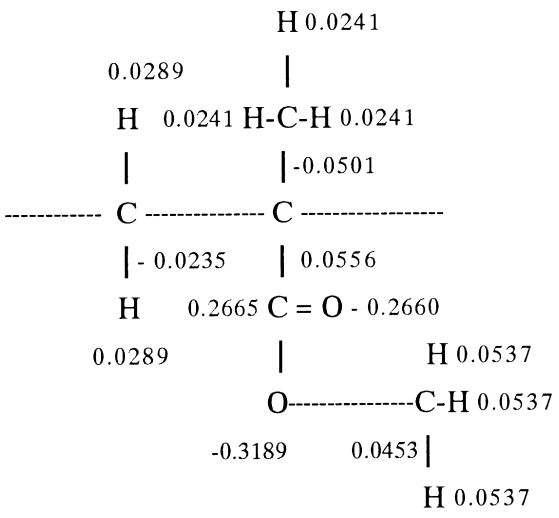

have these several unresolved problems, the model obtained in the energy calculation was used for the calculation of the three-dimensional elastic constants of the crystal in order to estimate, even roughly, the effect of the double-strand helical structure on the crystallite modulus.

3.2.2. Three-dimensional elastic moduli

The calculation of the elastic constants was made by using the software included in Cerius[2], the principle of which is to calculate the second derivatives of the potential energy with respect to the infinitesimally small strain or at the energetically-minimal point of the potential curve. The elastic constant C_{ij} corresponds to $(d^2V/d\varepsilon_i d\varepsilon_j)_o$ where V is the potential function and ε_i is the ith strain tensor component ($i = 1$–6) [22]. The obtained compliance tensor ($\mathbf{s}_{ij}$) and elastic constant (c_{ij}) matrices are shown below:

$$s_{ij}(10^{-2}/\mathrm{GPa}) = \begin{bmatrix} 5.02962 & -0.28279 & -1.87716 & -0.26734 & -0.04364 & -1.14367 \\ -0.28279 & 3.21109 & -1.66942 & 0.67670 & -0.88710 & -1.05807 \\ -1.87716 & -1.66942 & 5.22305 & 0.90338 & 3.34942 & 1.63928 \\ -0.26734 & 0.67670 & 0.90338 & 11.14020 & 3.86621 & 0.98566 \\ -0.04364 & -0.88710 & 3.34942 & 3.86621 & 17.93130 & -1.37448 \\ -1.14367 & -1.05807 & 1.63928 & 0.98566 & -1.37448 & 19.15850 \end{bmatrix}$$

$$c_{ij}(\mathrm{GPa}) = \begin{bmatrix} 25.31518 & 8.77982 & 12.85323 & -0.43046 & -1.75133 & 0.79280 \\ 8.77982 & 41.93949 & 16.77965 & -3.80541 & -0.09546 & 1.59350 \\ 12.85323 & 16.77965 & 33.11326 & -1.49585 & -5.11088 & -1.42905 \\ -0.43046 & -3.80541 & -1.49585 & 10.13604 & -2.15544 & -0.78398 \\ -1.75133 & -0.09546 & -5.11088 & -2.15544 & 7.05967 & 0.94486 \\ 0.79280 & 1.59350 & -1.42905 & -0.78398 & 0.94486 & 5.58534 \end{bmatrix}$$

The energy-minimized crystal structure is shown in Fig. 9 where the lattice parameters are $a = 23.62$ Å, $b = 13.34$ Å, $c = 10.84$ Å, $\alpha = 112.70°$, $\beta = 89.51°$ and $\gamma = 92.15°$. The obtained lattice parameters are, on the whole, bigger than those of the X-ray values. One important factor affecting the calculated result may be that the utilized potential parameters, in particular the parameters closely related with the intermolecular interactions of van der Waals and Coulombic interactions, were not sufficiently refined to give a good reproduction of the observed vibrational spectral data, for example. The reasonableness of the assigned atomic charges might be also one of the significant factors affecting the calculated structure. The refinement of the potential function parameters, as well as the atomic charges, should be made in the future, in order to give truly reasonable energy calculation results, including the simulation of the crystal structure at various temperatures. Although we still

where the Cartesian coordinates are defined in the following way: the 3 axis//the c axis and the 2 axis is in the bc plane. From the compliance matrix, the Young's modulus, E_c, along the chain direction was calculated to be $E_c = 1/\mathbf{s}_{33} = 19.1$ GPa, which is almost twice as high as the experimental value, ca. 10 GPa, observed at room temperature. The calculated value corresponds to the modulus of the crystal at 0 K and should be higher than that at room temperature because of the cessetion of the disordering caused by the molecular motion [14,15,23,24]. At the same time, the force field parameters are not refined, as stated above. Therefore, at the present stage, we may keep the calculated modulus as a rough estimation based on the energetically minimized structural model.

The *it*-PMMA takes the doubly-stranded helical form. In order to estimate the effect of intertwining the two helical chains on the crystallite modulus, we also calculated the

modulus for the crystal structure model consisting of single helical chains. Starting from the energy-minimized structure of Fig. 9, the crystal lattice was constructed by replacing the two double-stranded helices by single helices. This new crystal structure was optimized energetically. First it was relaxed by carrying out molecular dynamics at 500 K for 10 ps. Then the energy was minimized again. The chain conformation thus obtained is shown in Fig. 10 in comparison with that of the double-stranded helices. The lattice cell parameters are $a = 21.52$ Å, $b = 13.35$ Å, $c = 10.87$ Å, $\alpha = 119.80°$, $\beta = 90.35°$, and $\gamma = 88.26°$. The potential energy is about 374 kcal mol^{-1} unit cell^{-1} higher than that of the double-helix model, indicating the energetical preference of the double helix. The Young's modulus calculated for the single chain crystal is 11 GPa, about half the value for the double-stranded structure. In other words, the double-stranded structure gives a higher modulus because of the mechanical strengthening that results from the intertwining of the two chains of *it*-PMMA.

Apparently the value calculated for the single chain model, ca. 11 GPa, is rather close to the observed modulus. But we should not give such a simple conclusion that the single-strand helical structure is therefore more plausible as the reasonable chain conformation of *it*-PMMA. Judging from the above-mentioned various problems included in the quantitative theoretical estimation, as well as in the X-ray experiment, both the observed and calculated moduli should contain the errors of significant degree. The reasonableness of the double-stranded structural model, supported by both the X-ray structure analysis and the energetical stability, may make it preferable to compare the observed modulus with that calculated for the double helix. At the present stage of the calculation, we should notice only the important point that the intertwining of the two chains has an effect to give an appreciably higher Young's modulus along the chain axis than the single chain.

This increase in the modulus by the intertwining of two chains is considered to come from the non-bonded interatomic interactions between the contacting two chains. A similar situation can be found in the case of *n*-fatty acid single crystals. *n*-Fatty acid crystals show the phenomenon of polytype, where the adjacent layers are stacked together in different manners [25]. For example, when the chain packing in one layer is expressed as //////////////////// (/ denotes one chain or, more exactly, one dimer), the adjacent layers might be stacked in the following two different ways:

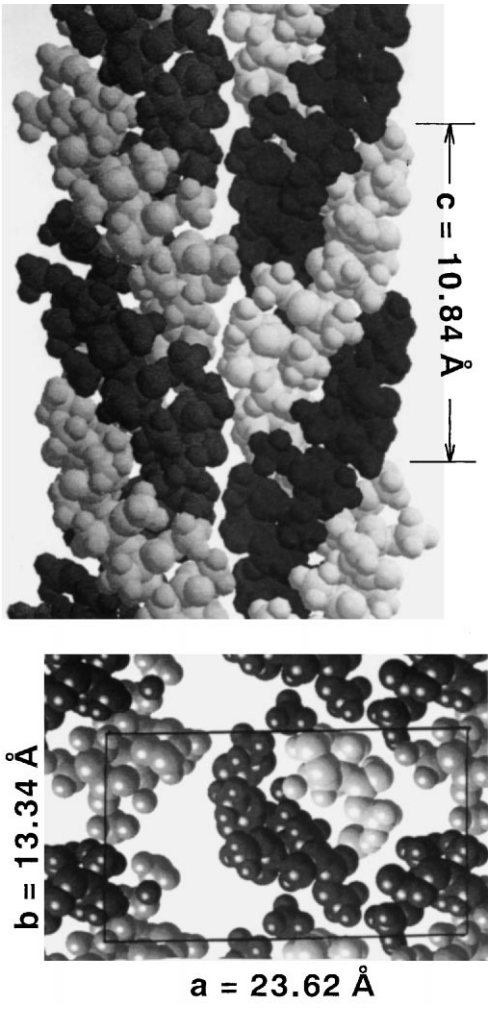

Fig. 9. Energy-minimized crystal structure of the *it*-PMMA double-stranded helices.

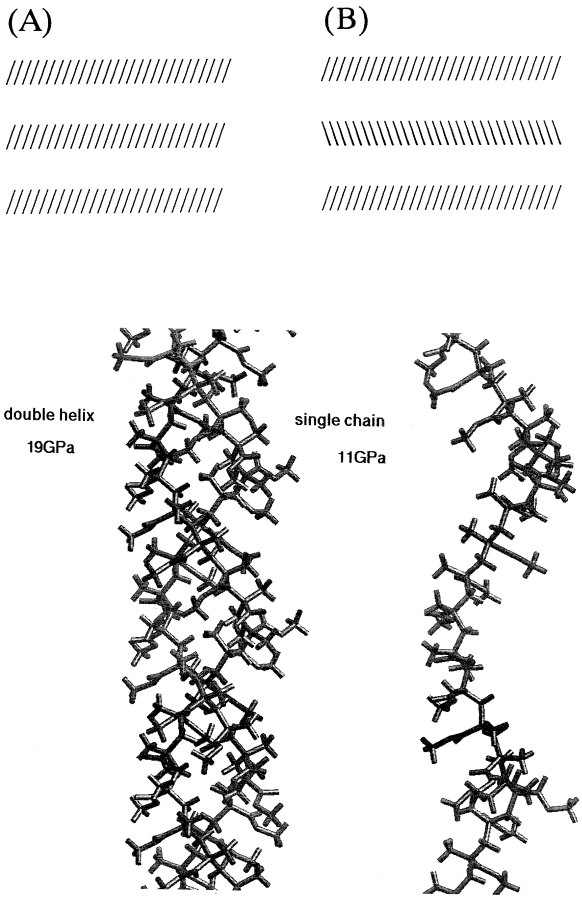

Fig. 10. Energy-minimized crystal structure of the single helix model of *it*-PMMA.

These two different stacking structures were reported to give the different Young's moduli along the normal to the layer plane: the modulus of structure (A) is twice as high as that of (B) [25]. This big difference in mechanical property comes from the difference in the deformation mechanism under the externally-applied tensile force. The adjacent layers are stacked together by weak interactions between the CH_3 end groups. The structures (A) and (B) show only slightly different interaction energies due to these weak intermolecular interactions. That is to say, these quite small intermolecular interactions may possibly affect the mechanical property of the crystal lattice remarkably. An effect of the intertwining of the two *it*-PMMA chains on the crystallite modulus along the chain axis may be interpreted in a similar way.

4. Conclusions

The crystallite modulus of *it*-PMMA along the chain direction was obtained by the X-ray diffraction method to be ca. 10 GPa. The computer simulation gave the modulus of ca. 19 GPa for the double-stranded helical model and ca. 11 GPa for the single chain. Although the calculated values seem to be overestimations, the calculation revealed the effect of the intertwining of the two chains on the mechanical toughening along the chain axis.

This work is a starting point for other matters of interest such as a possible comparative study on the Young's modulus of three types of PMMA crystal structures: *it*-PMMA; syndiotactic PMMA (*st*-PMMA); and the so-called stereocomplex between the *it*- and *st*-PMMA. These three types of crystal structure involve three different types of helices: a double-stranded helix for *it*-PMMA; a solvated large-radius single helix for *st*-PMMA [26]; and an *it*-PMMA chain surrounded by a *st*-PMMA chain in the case of the stereocomplex [27]. The experimental and theoretical evaluation of these substances are now being performed, the results of which will be reported as soon as possible.

References

[1] Stroupe JD, Hughes RE. J Am Chem Soc 1958;80:2341.
[2] D'Alagni M, De Santis P, Liquori AM, Savino M. J Polym Sci (B) 1964;2:925.
[3] Liquori AM, Anzuno Q, Coiro VM, D'Alagni M, De Santis P, Savino M. Nature (London) 1965;206:358.
[4] Coiro VM, De Santis P, Liquori AM, Mazzarella L. J Polym Sci (C) 1969;16:4591.
[5] Kusanagi H, Tadokoro H, Chatani Y. Macromolecules 1976;14:591.
[6] Bosscher F, Ten Brinke G, Eshuis A, Challa G. Macromolecules 1982;15:1364.
[7] Miller KJ. Macromolecules 1991;24:6877.
[8] Kusanagi H, Chatani Y, Tadokoro H. Polymer 1994;35:2028.
[9] Hatada K, Ute K, Tanaka K, Okamoto Y, Kitayama T. Polym J 1986;18:1037.
[10] Kitayama T, Ute K, Yamamoto M, Fujimoto N, Hatada K. Polym J 1990;22:386.
[11] Tashiro K, Nishimura H, Kobayashi M. Macromol Rapid Commun 1996;17:633.
[12] Sakurada I, Kaji K. J Polym Sci (C) 1970;31:57.
[13] Nakamae K, Nishino T, Hata K, Matsumoto T. Kobunshi Ronbunshu 1985;42:241.
[14] Tashiro K, Kobayashi M, Tadokoro H. Polym Engng Sci 1994;34:308.
[15] Tashiro K, Wu G, Kobayashi M. Polymer 1988;29:1768.
[16] Nakamae K, Nishino T, Hata K, Yokoyama F, Matsumoto T. Zairyo 1986;35:106.
[17] Tashiro K, Tadokoro H. Macromolecules 1981;14:781.
[18] Sawatari C, Matsuo M. Macromolecules 1986;19:2653.
[19] Tashiro K, Kobayashi M, Tadokoro H. Polym J 1992;24:899.
[20] Rappe AK, Casewit CJ, Colwell KS, Goddard III WA, Skiff WM. J Am Chem Soc 1992;114:10024.
[21] Gasteiger J, Marsili M. Tetrahedron 1980;36:3219.
[22] Rutledge GC, Suter WU. Polymer 1991;32:2179.
[23] Tashiro K, Kobayashi K. Polymer 1996;37:1775.
[24] Tashiro K, Kobayashi K. Rep Progr Polym Phys Jpn 1996;39:349.
[25] Ito Y, Kobayashi M. J Chem Phys 1991;95:1794.
[26] Kusuyama H, Miyamoto N, Chatani Y, Tadokoro H. Polym Commun 1983;24:119.
[27] Schomaker E, Challa G. Macromolecules 1989;22:3337.